ACS APPLIED MATERIALS & INTERFACES

www.acsami.org Research Article

Multifunctional Dental Composite with Piezoelectric Nanofillers for Combined Antibacterial and Mineralization Effects

Carolina Montoya, Anubhav Jain, Juan José Londoño, Santiago Correa, Peter I. Lelkes, Mary Anne Melo, and Santiago Orrego*

Cite This: *ACS Appl. Mater. Interfaces* 2021, 13, 43868–43879 Read Online

ACCESS | Metrics & More | Article Recommendations | Supporting Information

ABSTRACT: After nearly seven decades of development, dental composite restorations continue to show limited clinical service. The triggering point for restoration failure is the degradation of the bond at the tooth–biomaterial interface from chemical, biological, and mechanical sources. Oral biofilms form at the bonded interfaces, producing enzymes and acids that demineralize hard tissues and damage the composite. Removing bacteria from bonded interfaces and remineralizing marginal gaps will increase restorations' clinical service. To address this need, we propose for the first time the use of piezoelectric nanoparticles of barium titanate ($BaTiO_3$) as a multifunctional bioactive filler in dental resin composites, offering combined antibacterial and (re)-mineralization effects. In this work, we developed and characterized the properties of dental piezoelectric resin composites, including the degree of conversion and mechanical and physical properties, for restorative applications. Moreover, we evaluated the antibacterial and mineralization responses of piezoelectric composites *in vitro*. We observed a significant reduction in biofilm growth (up to 90%) and the formation of thick and dense layers of calcium phosphate minerals in piezoelectric composites compared to control groups. The antibacterial mechanism was also revealed. Additionally, we developed a unique approach evaluating the bond strength of dentin–adhesive–composite interfaces subjected to simultaneous attacks from bacteria and cyclic mechanical loading operating in synergy. Our innovative bioactive multifunctional composite provides an ideal technology for restorative applications using a single filler with combined long-lasting nonrechargeable antibacterial/remineralization effects.

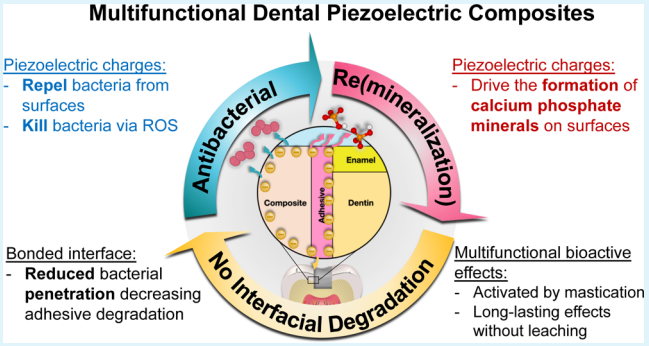

KEYWORDS: *antibiofilm, antibacterial, multifunctional, resin composite, barium titanate, calcium phosphate, biofilms, dental caries, nanoparticles, bioactive, nanofillers*

Downloaded via TEMPLE UNIV on August 31, 2023 at 17:14:45 (UTC).
See https://pubs.acs.org/sharingguidelines for options on how to legitimately share published articles.

1. INTRODUCTION

The oral cavity is a harsh and complex environment that poses significant challenges to the clinical success of dental restorations.[1] Secondary caries is considered as one of the leading causes of failure of resin composite restorations,[2,3] which is currently the most used restorative biomaterial.[4] The clinical service life of composite restorations is less than 10 years, with more than 50% of procedures requiring replacement.[3] With the phase-down mandate of dental amalgams,[5] the number of composite restorations is expected to grow. Thus, it is necessary to find novel approaches that improve the durability of composite restorations.

Dental resins are degraded by enzymes sourced from saliva and bacteria[1] and by acids produced by bacteria.[6] In addition, bacterial activity is upregulated by the release of unreacted monomers.[7] Collagen in dentin is degraded by the activation of collagenase matrix metalloproteinases (MMPs),[8] and calcium phosphate minerals are eroded after acid exposure.[9] Also, the bonded interface can be weakened by repetitive masticatory forces,[10] thermal cycling,[11] and the elastic mismatch of bonded materials.[12] These factors could work in synergy to degrade the restoration bond's strength, which may facilitate the progression of secondary caries and induce restoration failure.[2] Besides, there is a lack of experimental approaches to evaluate the bonding strength of restorations simulating the problematic bacteria- and enzyme-rich environment working in synergy, which impedes the elucidation of disease mechanisms and the assessment of new materials, especially bioactive ones.[1]

Reducing the acid attack on the biomaterial surfaces at the bonded interfaces is necessary to prevent composite restorations' early failure. The addition of antibacterial and

Received: April 7, 2021
Published: September 8, 2021

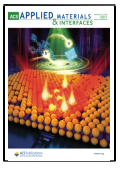

© 2021 American Chemical Society

https://doi.org/10.1021/acsami.1c06331
ACS Appl. Mater. Interfaces 2021, 13, 43868–43879

(re)mineralization bioactive agents has been proposed as the relevant strategy to address this challenge.[13,14] Removing pathogenic bacteria inhibits the production of bacterial acids/enzymes, while the formation of new minerals may enable the healing of gaps/defects at the bonded interface. Existing antibacterial/antibiofilm agents include leachable compounds (*e.g.*, chlorhexidine), polymerizable monomers (*e.g.*, quaternary ammonium methacrylate, zwitterion, and ester-free resins), antibacterial peptides (AMPs), and filler nanoparticles (*e.g.*, silver and zinc).[1,15,16] Two major limitations of current antibacterial technologies include the short duration of the antibacterial effect due to the exhaustion of antibacterial agent release and the inability to regenerate the loss of mineral content from the hard dental tissue damage.

On the other hand, multiple (re)mineralizing agents have been proposed,[17] including nanofillers (*e.g.*, amorphous calcium phosphates and calcium fluoride) and cationic monomers (*e.g.*, pyromellitic glycerol dimethacrylate).[18,19] Common limitations of remineralizing technologies include the need for a base mineral as a seeding site and the slow growth rate of new minerals.[20] Recently, multifunctional dental composites, including both antibacterial and remineralizing agents, have been proposed to overcome some limitations of individual formulations.[21,22] Despite their extraordinary potential, these materials are generally expensive, with complex synthesis and formulations limiting the tunability of bioactive properties for clinical use.

Piezoelectric materials generate electric charges in response to an applied mechanical load. This class of materials has been successfully used in different biomedical applications, including bone regeneration, drug delivery, and tissue engineering.[23] Dentistry has not yet fully benefited from the different therapeutical effects offered by piezoelectric materials. Our recent work showed that piezoelectric charges offer bioactivity by forming mineral layers proportional to the electrical charge.[24] Dentistry will benefit from this technology since certain piezoelectric materials produce sustained electrical charges for more than 12 million cycles of mechanical loading/unloading,[25] which would correspond to ~24 years of clinical service, assuming an average of 500k mastication cycles per year.[26] Recent work showed that the electrical polarization of piezoelectric materials could offer antibacterial effects.[27−30]

Little is known about the antibacterial effects of piezoelectric charges and piezoelectric materials for dental applications. These combined antibacterial and mineralization therapies are ideal for improving the bond of composite restorations by concomitantly removing pathogenic bacterial species and forming new minerals for extended periods of time at the restoration margin.

The aim of this study is twofold: to systematically investigate the antibacterial and mineralization effects of piezoelectric dental composites and to evaluate the bond strength of piezoelectric composites after being challenged by the synergy of bacterial attacks and cyclic loading. We characterized the mechanical/physical properties, evaluated the antibacterial/antibiofilm and remineralization effects, and assessed the bond strength.

2. MATERIALS AND METHODS

2.1. Fabrication of Piezoelectric Composite Samples. The piezoelectric resin composite was fabricated by mixing standard dental resins with nanoparticles of BTO (US Nanomaterials US3830, 200 nm) and silanized barium boroaluminosilicate glass fillers (median diameter of 1.4 μm, Dentsply Caulk).[22] Briefly, bisphenol A diglycidyl dimethacrylate (Bis-GMA) (Sigma 494356) and triethylene glycol dimethacrylate (TEGDMA) (Sigma 261548) resins were mixed in a 1:1 ratio by weight using a magnetic stirrer at 60 °C for 30 min. Camphorquinone (CQ) (Sigma 124893) and ethyl 4-dimethylaminobenzoate (4E) (Sigma E24905) were added as the initiator and co-initiator in proportions of 0.2 and 0.8 wt % of the resin, respectively.

The blend was mixed with 70% (wt/wt) fillers, defined as the maximum packing fraction. This value was kept constant among all groups to avoid inconsistencies in the resin/filler ratio. Fillers were distributed between BTO nanoparticles in different ratios including 1% (which renders a final concentration of 0.2% Ti and 0.6% Ba), 10% (1.8% Ti−5.35% Ba), and 60% (7.7% Ti and 22% Ba) (wt/wt) and complemented by the barium borosilicate glass filler.

The control group was prepared without BTO fillers. Mixing was conducted using a planetary mixer (Thinky ARE-310) for 1 min at 2000 rpm. The liquid mixture was then poured into a mold with the desired sample shape. The mixture was light-cured with a LED unit (Cure TC-3, Spring Health Products). The mold's top and bottom surfaces were irradiated for 1 min on each side, resulting in a total radiant exposure of 166 J/cm^2 (equivalent to 1 min at 980 mW/cm^2). After curing, the average roughness of the surfaces was verified as <0.2 μm (see Supporting Information-1). To align the electric dipole and increase the electrical conversion, samples were subjected to a high electric field (20 kV/mm) at 140 °C for 40 min (poling).[31] Then, samples were stored in distilled water for 24 h at 37 °C for the release of unreacted monomers before testing.

2.2. Piezoelectric Composite Characterization. A thorough characterization of the piezoelectric composite properties was conducted, including the morphological and chemical composition (Supporting Information-2), mechanical response (Supporting Information-3), electromechanical (piezoelectric) performance (Supporting Information-4), degree of conversion (DC) (Supporting Information-5), water sorption/solubility (Supporting Information-6), and dimensional change (Supporting Information-7).

2.3. *In Vitro* Biofilm Model. *2.3.1. Bacterial Strain and Culture.* We developed a single-species biofilm *in vitro* model to evaluate the piezoelectric composite's antibacterial activity.[22,32] *Streptococcus mutans* was selected due to the bacteria's high association with dental caries and virulence. This caries-related pathogen can utilize dietary carbohydrates (sucrose) to synthesize extracellular polysaccharides (EPS). Its acidogenic and aciduric properties inhibit commensal species and degrade resin composites *via* hydrolysis.[33] The strain (ATCC 25175) was plated in a brain−heart infusion (BHI) agar plate and incubated at 37 °C for 24 h. A single colony was harvested and incubated overnight in fresh BHI stirred at 130 rpm. The solution was diluted in fresh BHI to obtain OD_{600} = 0.1 (~10^6 cfu/mL) (Figure 2a). The final solution was supplemented with 2% sucrose to represent a low sugar diet.[34] Rectangular beams (5 × 1 × 18 mm^3) were sterilized with a 15 min immersion in 70% ethanol and air-dried inside a biological safety cabinet during UV light exposure.

The beams were submerged in 3 mL of the diluted liquid culture with the negatively charged surface oriented upward (*i.e.*, compression side). To allow bacterial adhesion to the material surfaces, samples were incubated statically at 37 °C for 2 h. The samples were then gently washed (3×) with phosphate-buffered saline (PBS) to remove unattached cells. Samples were placed in a 3-point bending fixture (span: 15 mm) with new media. Repetitive (cyclic) loading was initiated at 2 Hz throughout the incubation period. The load magnitude was adjusted to resemble a stress range found in clinical settings for dental restorations (~40 MPa).[35] The medium was removed after the incubation period (24 h). The tension side and borders of the beams were gently cleaned using a cell scraper. Samples (N = 7 per group per evaluation) were gently rinsed with PBS to remove unattached cells and utilized to evaluate the biofilm−biomaterial interactions.

2.3.2. Biofilm Biomass and Metabolic Activity. To assess the biomass and metabolic activity of the biofilms, crystal violet (CV) and MTT [3-(4,5-dimethylthiazol-2-yl)-2,5-diphenyltetrazolium bromide][36] assays were employed, respectively. For biomass measure-

https://doi.org/10.1021/acsami.1c06331
ACS Appl. Mater. Interfaces 2021, 13, 43868−43879

ments, samples were stained with 1 mL of 0.1% CV (Sigma V5265) at room temperature for 20 min. As a de-staining solution, acetic acid 30% (v/v) (Ricca Chemical 1383032) was added to the samples and shaken by hand at room temperature until the biofilm was dissolved. For MTT measurements, samples were incubated with 0.5 mg/mL MTT solution (Thermo Fisher Scientific V13154) at 37 °C. After 2 h, the MTT solution was replaced with an equal amount of dimethyl sulfoxide (DMSO) (Sigma BP231100) and shaken by hand in the dark until all formazan crystals were completely dissolved. For both tests, aliquots (125 μL) were transferred to a 96-well plate. Absorbances at 550 nm (A_{550}) and 540 nm (A_{540}) were measured for the quantification of biomass and metabolic activity, respectively, (BioTEK Synergy HTX). The absorbance values were normalized to the compression side of the samples (the surfaces where the biofilms were studied). Biofilms cultured inside an empty well filled with 3 mL of the diluted bacteria culture were defined as positive controls. This standardization is recommended as routine practice.[36] The absorbance values were normalized to the surface area of the 12-well plate. The biofilm biomass and metabolic activity were expressed as a percentage of the positive control group as[36]

$$\% \text{ Control} = \left(\frac{\dfrac{A_{550} \text{ sample}}{\text{surface area for biofilm growth}}}{\dfrac{A_{550} \text{ positive control}}{\text{area of the bottom surface of the well}}} \right) \times 100 \quad (1)$$

2.3.3. Colony-Forming Units. The bacterial viability was assessed by counting the number of colony-forming units (cfu). To detach the biofilm from the biomaterial surface (compression side), samples were sonicated for 1 min at 40 kHz and then vortexed for 30 s in 1 mL of PBS. Six 10-fold serial dilutions were prepared, and 50 μL of each solution was plated on BHI agar plates and incubated for 24 h at 37 °C. The number of colonies was then counted manually and normalized with the positive control and the sample's surface area for bacterial growth (see eq 1).

2.3.4. Live/Dead Fluorescent Microscopy. *S. mutans* biofilms were observed using confocal laser scanning microscopy (CLSM) (Olympus Corporation, FV1200). Cells were stained using a LIVE/DEAD BacLight bacterial viability kit (Thermofisher Scientific L7007) according to the manufacturer's instructions. A solution of fluorescent stain was prepared by mixing 3 μL of SYTO9 and 3 μL of propidium iodide (PI) in 1 mL of ultrapure water. Aliquots (200 μL) of the staining solution were applied to the sample surface and incubated in a dark room for 20 min. Samples were gently rinsed with filter-sterilized water to remove the excess dye. A dry 10× objective was used to visualize the biofilms. The laser was set at 488 nm (excitation wavelength), while the emission was observed at 528 nm for SYTO9 (green) and 645 nm for PI (red). Confocal images with a resolution of 1024 × 1024 pixels were taken on the compression side of the beam. All images and stacks were captured with identical pinholes and gain settings. Biofilms were reconstructed using Image J with the 3D viewer plug-in. The biofilm volume was quantified using Comstat2.

2.3.5. Reactive Oxygen Species. Reactive oxygen species (ROS) production was evaluated to assess the potential antibacterial mechanism of piezoelectric charges.[37] To detect oxidative stress, samples (N = 3 for each group) were stained with 5 μM CellROX Green reagent (Thermo Fisher Scientific C10444) and incubated at 37 °C for 30 min according to the manufacturer's instructions. Samples were then carefully rinsed with PBS. ROS accumulation was quantified using a fluorescence plate reader at excitation/emission 485/535 nm wavelengths (BioTEK Synergy HTX).

2.4. Mineralization Model. To evaluate the formation of new minerals on piezoelectric composites from calcium-saturated media, an *in vitro* model was developed as described.[24] Rectangular beams (5 × 1 × 18 mm^3) of piezoelectric composites (N = 3 per group) were submerged in calcium-saturated solutions with a composition of calcium ions similar to that found in body fluids (*e.g.*, dentinal fluid).[38] A 10 times concentrated simulated body fluid (10× SBF) was prepared by dissolving reagent-grade NaCl, $NaHCO_3$, KCl, $MgCl_2 \cdot 6H_2O$, $CaCl_2 \cdot 2H_2O$, and $NaH_2PO_4 \cdot H_2O$ (all from Sigma-Aldrich) in deionized water[38] (for details, see Supporting Information-8). Samples maintained in SBF were subjected to repetitive loading (3-point bending at 2 Hz, span 15 mm) at 37 °C (Figure 3a). The 10× SBF solution was refreshed every two days to replenish the calcium ions. Two simulated body solutions were utilized, including 1× SBF for 14 days and 10× SBF for 7 days (Supporting Information-8).[38]

After the incubation period, samples were immersed overnight in deionized water to remove soluble inorganic ions. The quantity, morphology, and chemistry of the formed minerals on the negative side of the beam were characterized. Scanning electron microscopy (SEM) and energy-dispersive X-ray spectroscopy (EDS) were utilized to visualize and evaluate the mineral's constituting elements. A contact profilometer (Surfcorder SE 1700) was used to quantify the step height (thickness) of the new mineral layer formed. The step height (Ry) was measured by calculating the difference between the peaks and valleys of the surface profile after masking the sides of the material surface. Several lines were measured along with different locations of the mineral layer.

2.5. Synergistic Degradation of the Bonded Interfaces. *2.5.1. "Twin-Interface" Sample Preparation.* To study the degradation of the dentin−adhesive−composite interfaces, twin-interface samples (Figure 4a) were prepared, as described previously.[22] Noncarious extracted molars (20 years < age < 33 years) were obtained from the Kornberg School of Dentistry clinic. The teeth were sectioned (Leco VC-50) to obtain dentin blocks (2 × 2 × 2 mm^3). The sections were consistently derived from the mid-coronal region to avoid tubule density and mineral/collagen ratio variations. Dentin blocks were transferred to a mold with the occlusal surface facing upwards, so that composites were bonded on the mesial and distal sides (Figure 4a). The etch-and-rinse technique was employed to bond dentin with an adhesive/composite system, mimicking clinical procedures.

First, the mesial and distal proximal sides of dentin were etched with 32% phosphoric acid for 15 s and rinsed with water for 10 s. Then, one layer of adhesive (3M Scotchbond Universal Adhesive) was applied over the etched surface, followed by air drying for 5 s and light curing for 20 s (following the manufacturer's instructions). After applying the adhesive layer, the resin composite ("bulk") was added in 1 mm layers; each layer was irradiated for 40 s. Four layers of the composite were required on each side of the dentin block. The bulk resin was prepared for the control group by mixing Bis-GMA/TEGDMA with 70% wt of the boroaluminosilicate glass fillers (Section 2.1). The adhesive was added with 5% wt BTO (US Nano US3835, 50 nm) and the bulk resin was added with 10%wt of BTO (Nano US3830, for the piezoelectric group 200 nm). Before tests, samples were immersed in Hank's balanced salt solution (HBSS) for 24 h.

2.5.2. Model for the Synergetic Degradation of the Bonded Interfaces. To replicate the oral conditions and adequately elucidate the antibacterial and remineralization effects of the piezoelectric charges on the bonding strength, media that included bacteria and calcium ions were prepared. Media with these characteristics have been previously used.[39] The media were prepared by combining liquid media of *S. mutans* (Section 2.3.1) and 10× SBF (Section 2.4) in ratios of 35% and 65% v/v, respectively, to a final volume of 45 mL. This combination did not affect the metabolic activity of the bacteria (Supporting Information-9). The media were supplemented with 5% sucrose and contained ∼3.5 × 10^5 cfu/mL, corresponding to the average number of *S. mutans* found in saliva.[40] A 2 h bacterial adhesion period was allowed before cyclic loading was initiated. The dentin−adhesive−composite interfaces were challenged by bacterial attacks and cyclic mechanical loading working in concert for 6 days. Twin-interface beams were loaded in a 4-point bending configuration (span: 20 mm) at 2 Hz and a stress ratio of R = 0.1.[41] The stress amplitude (σ_a) was set to 2 MPa, which is 25% of the endurance limit (6.5 MPa) reported for this degradative configuration.[22] The test was conducted for ∼1 M cycles, pulsing 1 mL of a 5% sucrose solution three times a day to represent dietary intake.[39] The media were replaced every 24 h, and the pH levels were measured every 15 min. After the challenge, the beam was removed, and the residual bond

https://doi.org/10.1021/acsami.1c06331
ACS Appl. Mater. Interfaces 2021, 13, 43868−43879

strength was immediately measured under quasi-static conditions (Supporting Information-3). To visualize bacterial penetration along the biointerfaces, confocal microscopy (Section 2.3.4) was performed on the fracture surface.

2.6. Statistical Analysis. For all evaluations, statistical differences were obtained using one-way ANOVA with a significance of 0.05. The ANOVA assumption of normal distribution was assessed by Shapiro–Wilk's test, and the assumption of homoscedasticity was done by Levene's test. The Tukey post-hoc test was used for multiple comparisons with a 95% confidence level. All statistical analyses were completed using STATGRAPHICS Centurion XVII.

3. RESULTS

3.1. Piezoelectric Composite Characterization. Piezoelectric fillers were observed to be evenly distributed along with the resin matrix in small agglomerates (Figure 1a). Elemental analysis confirmed the presence of barium and titanium corresponding to the composition of the BTO and peaks of Si and Al corresponding to the boroaluminosilicate fillers' composition (see Figure 1b). Overall, the addition of BTO resulted in a decrease in the mechanical properties compared to the control (Figure 1c,d). The average flexural strength of the piezoelectric composites with 1 and 10% BTO was similar (~65 MPa) and higher than that for composites with 60% BTO (~26 ± 4.4 MPa); the flexural strength of all piezoelectric composites was statistically lower ($p \leq 0.05$) than that of the composite control (74 ± 5.2 MPa). The flexural modulus of piezoelectric composites ranged between ~2 and 3.8 GPa and was significantly lower than that of the control (~4.1 ± 0.6 GPa). The charge density (electrical charge per surface area) was proportional to the amount of the piezoelectric filler (Figure 1e). A more detailed electromechanical characterization is presented in Supporting Information-4. As expected, no electrical charge was measurable in the control composite (no BTO filler). The DC values of all evaluated composites were statistically indistinguishable with an average of 83% ($p > 0.05$) (Figure 1f).

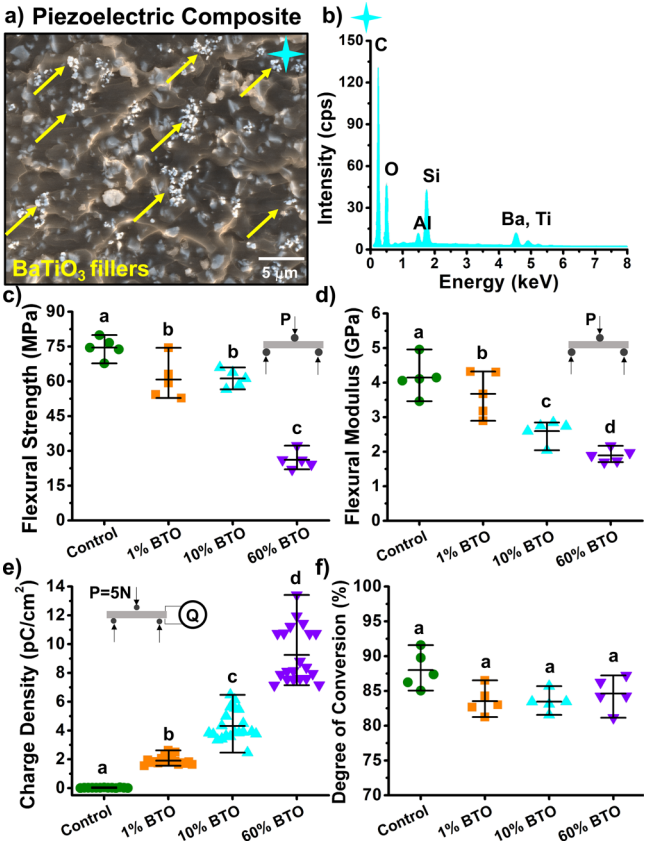

Figure 1. Characterization of piezoelectric composites. (a) Micrograph of the fracture surface of a 10% BTO composite. Yellow arrows show piezoelectric fillers. (b) Representative EDS spectrum of the fracture surface of a 10% BTO composite showing peaks corresponding to barium and titanium of the BTO, while the Si and Al peaks reflect the composition of the boroaluminosilicate filler. The spot marked in (a) corresponds to the location where the EDS spectrum was taken. (c) Flexural strength of the piezoelectric and control dental composites. (d) Flexural modulus of the piezoelectric and control dental composites. (e) Electrical charge density (charge per area) of resin composites after being subjected to a three-point bending cyclic load of 5 N at 2 Hz. (f) Degree of conversion (DC) of composites evaluated by attenuated total reflection Fourier transform infrared spectroscopy (ATR–FTIR). $N = 5$ for each evaluation. Horizontal lines correspond to the minimum, mean, and maximum values. Means with different letters are significantly different from each other ($p \leq 0.05$).

3.2. Biofilm–Biomaterial Interactions. The biofilm–biomaterial interactions were evaluated by measuring the biofilm biomass and the metabolic activity by counting the number of viable cells and reconstructing the biofilm volume. First, we explored whether the polarization of the piezoelectric composites had antibacterial effects (samples under no cyclic loading). All parameters studied (biomass, metabolic activity, and cfu) of the control and piezoelectric composites were statistically similar in the absence of cyclic loading (Figure 2b). A uniform biofilm layer (~30 μm thick) was observed for the control composite, whereas dispersed agglomerations of bacteria were observed for the piezoelectric composites (Figure 2c). The quantity (volume) of the biofilm for both groups was similar.

Second, we explored the effects of piezoelectric charges on the antibacterial effect by applying cyclic loading to the samples throughout the culture period. All the above-mentioned parameters (biomass, metabolic activity, and cfu) for the piezoelectric composites with 10% BTO at 3.2 pC/cm^2 of electrical charge were statistically lower than those for the control group ($p \leq 0.05$) (Figure 2d). Importantly, no biofilm layer was formed at the surface of the piezoelectric composite (Figure 2e). By contrast, a uniform and thick biofilm layer was formed in the control group under mechanical loading, similar to that of the no-load group.

Third, we evaluated the effects of the concentration of the BTO filler and the magnitude/polarization of electrical charges on the observed antibacterial effects of our composites (Figure 2f). Overall, a lower magnitude of charge and BTO content elicited increased antibacterial effects. With a fixed magnitude of electrical charge ($Q = 1.2$ pC/cm^2), a higher BTO content showed increased metabolic activity, but this was still significantly lower than the positive control [Figure 2f(1)]. With a fixed amount of BTO (60%), a lower magnitude of electrical charges yielded a decreased metabolic activity (improved antibacterial effect) [Figure 2f(2)]. The opposite was found for composites with 1% of BTO. The highest metabolic activity (least antibacterial effect) was evident when bacteria were grown on the positively charged surface yielding a 50% reduction compared with the positive control [Figure 2f(3)]. Moreover, the intracellular levels of ROS produced by the biofilms (indicative of oxidative stress) were significantly

https://doi.org/10.1021/acsami.1c06331
ACS Appl. Mater. Interfaces 2021, 13, 43868–43879

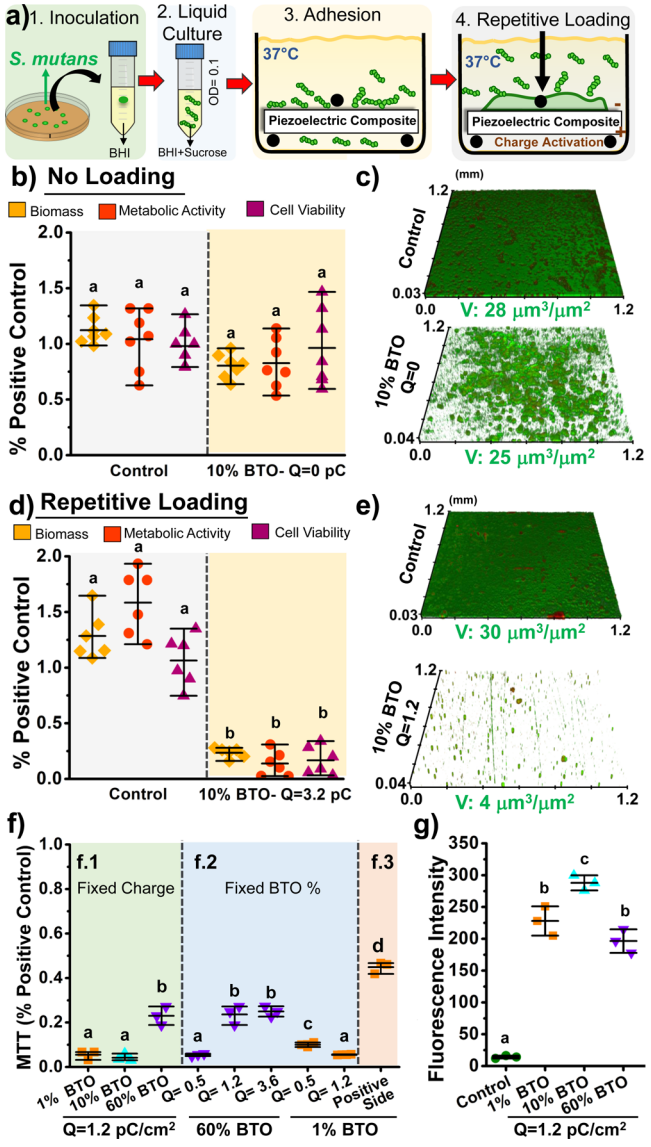

Figure 2. Single-species biofilm–biomaterial interactions. (a) Schematics of the *in vitro* model developed to cultivate biofilms on samples subjected to simultaneous liquid bacteria and repetitive mechanical loading. (b) Biofilm–biomaterial evaluations for the control and piezoelectric composites with 10% filler content without repetitive loading, including biofilm biomass, metabolic activity, and viable cell numbers. (c) Representative CLSM images of *S. mutans* biofilms on control and piezoelectric composites with 10% filler content without repetitive loading. Samples in (c) and (e) were stained with Syto-9 (green) and propidium iodide (red) to indicate live and dead bacteria, respectively. (d) Biofilm–biomaterial evaluations for the control and piezoelectric composites with 10% filler content under repetitive loading. As a positive control, biofilms cultivated inside an empty well were used. (e) Representative CLSM images of *S. mutans* biofilms on control and piezoelectric composites with 10% filler content and under repetitive loading. Tests were made applying a mechanical load of 5 N at 2 Hz, which corresponds to a generated electrical charge of 3.2 pC/cm^2. (f) Metabolic activity of *S. mutans* biofilms on samples with different amounts of BTO, magnitudes, and signs of electrical charge. (g) CellRox fluorescence intensity measured in *S. mutans* biofilms exposed to repetitive loading at 2 Hz. The electrical charge generated was 1.2 pC/cm^2 for each sample. The fluorescence intensity is proportional to the amount of intracellular ROS. N = 3–7 samples for each evaluation. Horizontal lines correspond to the minimum, mean, and maximum values. Means with different letters are significantly different ($p \leq 0.05$).

higher for the piezoelectric composites when compared to the control (Figure 2g).

3.3. Mineralization. Overall, calcium phosphate minerals were preferentially formed on the piezoelectric composites' negative surface after cyclic loading was engaged throughout the incubation period (Figure 3b). A 11.6 ± 4.1 μm-thick mineral layer was formed on the piezocomposites with 60% BTO at a charge of 1.2 pC/cm^2 after 7 days in 10× SBF. The mineral layer thickness was on average ~5 μm for the control and piezoelectric composites in the absence of cyclic loading. It appears that both the higher magnitude of electrical charges and BTO content favored mineralization (increased quantity of formed minerals) (Figure 3c). A charge of 3.2 pC/cm^2 yielded a mineral layer of 23.1 ± 3.7 μm thickness for 60% BTO.

Moreover, mineralization was independent of the calcium-saturated media (Figure 3d). After being submerged in 1× SBF for 14 days, a mineral layer of 22.6 ± 6.2 μm thickness was measured for the loaded piezoelectric composites with 60% BTO (Q = 3.2 pC/cm^2), which is similar to the quantity of minerals formed after 7 days in 10× SBF. No statistical difference was found in the mineral height between the positively charged surface of the piezoelectric composite and control groups. Micrographs revealed a distinctive dense layer of minerals formed on the negative surface of loaded piezoelectric composites (Figure 3e). The elemental analysis confirmed the presence of calcium phosphate minerals with a Ca/P ratio of 1.86 (Figure 3f), as expected for highly concentrated solutions (*i.e.*, 10× SBF).[42] Differently, minerals deposited on the control/loaded groups are dispersed spheroid particles with a diameter of up to 1 μm (Figure 3g) and a Ca/P ratio of 1.64 (Figure 3h), indicating less mineralization capability.

3.4. Bonding Strength of Degraded Biointerfaces. Bacterial penetration and bonded interfaces subjected to simultaneous degradative challenges were assessed by visualizing live/dead bacteria on the fractured surfaces. Cyclic loading enabled bacteria to access and colonize the adhesive/dentin interface in the control group (Figure 4b). A higher concentration of microorganisms was observed in the tensile stress region (Figure 4b). On the contrary, no significant number of bacteria penetrated the adhesive–dentin interface of piezoelectric composites (Figure 4c). The bacterial penetration for samples with no loading is presented in Supporting Information-10. The bacterial load covering the fracture surface was calculated for all tested groups (Figure 4d). Overall, a significantly higher bacterial growth was found in the control groups than in the piezoelectric composites under both loading conditions. The highest bacterial coverage (70% of the fracture surface) was observed under cyclic loading for the control group samples. The least bacterial coverage (14%) was observed in the piezoelectric composite samples under cyclic loading.

The residual bonding strength of composites of both groups before and after the degradation challenges is presented in Figure 4e. The highest bond strength (~33 MPa) was observed in both groups for samples right after preparation (no degradation challenges). However, after the 6-day challenge in bacterial load and/or cyclic mechanical loading, the bonding strength was significantly reduced by ~30% for all groups. No statistical differences were observed after comparing the samples subjected to combined bacterial and cyclic loading with those only subjected to bacterial challenges.

https://doi.org/10.1021/acsami.1c06331
ACS Appl. Mater. Interfaces 2021, 13, 43868–43879

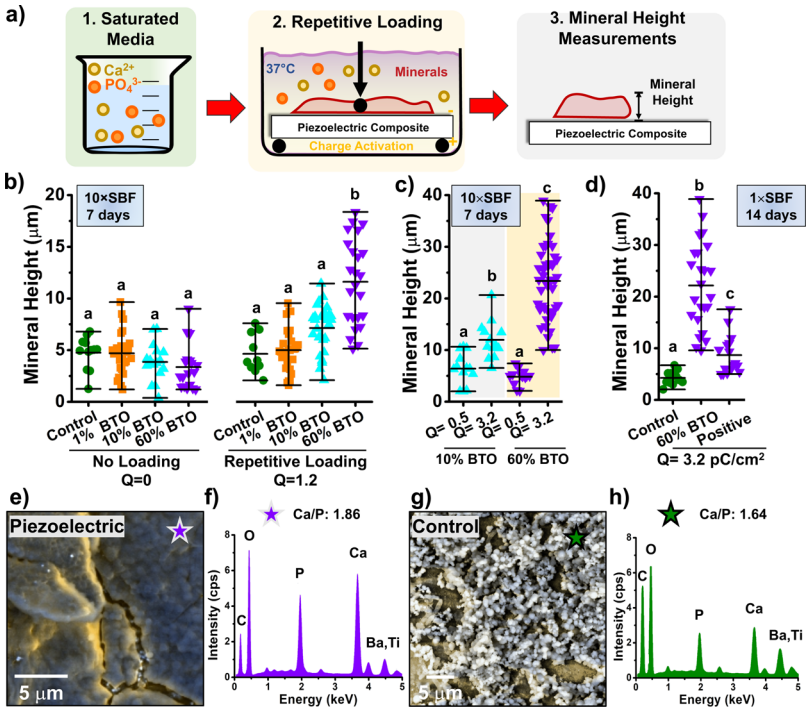

Figure 3. Mineralization effects of piezoelectric resin composites. (a) Schematics of an *in vitro* model to grow and measure minerals on samples subjected simultaneously to supersaturated solutions of simulated body fluid and repetitive mechanical loading. (b) Height of the minerals formed on the surface of the different groups tested. Tests were made applying a mechanical load that corresponds to an electrical charge of 1.2 pC/cm^2. (c) Height of minerals formed on samples with different amounts of BTO and magnitudes of electrical charges. (d) Effect of the media used (1× SBF or 10× SBF) and charge sign on the height of minerals on top of piezoelectric composites. $N = 3$ samples for each group; several measures were made along with different locations of the mineral layer. Horizontal lines correspond to the minimum, mean, and maximum values. Means with different letters are statistically different ($p \leq 0.05$). (e) Representative SEM micrograph of the minerals formed on the surface of the control composite. (f) EDS analysis obtained from a randomly selected region of the minerals formed on the control samples. (g) SEM micrograph of the minerals formed on the negative surface of a piezoelectric composite filled with 60% BTO. (h) EDS analysis of a randomly selected region of the mineral layer formed on the surface of a piezoelectric composite filled with 60% BTO and tested under mechanical loading.

The metabolic activity of the biofilms on the tension side is presented in Figure 4f. The lowest activity was measured for the piezoelectric composite group under cyclic loading. In addition, changes in the media's pH level during the 6-day challenge are presented in Figure 4g. After 24 h and the first change of media, both groups' pH decreased rapidly below 5.0 and remained near this value until the following medium change. The pH value was below 6.5 and 5.5 for 96 and 78 h, respectively.

4. DISCUSSION

In this work, we revealed for the first time that piezoelectric charges could be used as a novel material to remove pathogenic bacteria and form new calcium phosphate minerals over dental resin composites. Our findings unlock novel functionalities of piezoelectric materials for biomedical applications. These materials offer several advantages such as long-term delivery of therapeutic effects, no concern over the increased bacterial resistance to drugs, no leaching of the compounds, biocompatibility,[43] low cytotoxicity[44] (Supporting Information-11), and white coloring for aesthetics. Our work shows that a single compound can exert combined therapeutical effects and explored using a novel framework to show the effect of these functionalities on the bond strength of dental interfaces. The proposed approach enabled us to study, for the first time, the degradation of the bonded interfaces attacked in synergy by different chemical, biological, and mechanical sources, which will bring the field one step closer to having *in vitro* models representing clinical cases.

4.1. Antibacterial Effects of Piezoelectric Resin Composites. The antibacterial effects elicited by different ferroelectric/piezoelectric biomaterials such as BTO, zinc oxide, and PVDF against both Gram-positive (*Staphylococcus aureus*) and Gram-negative (*Pseudomonas aeruginosa* and *Escherichia coli*) bacteria have recently been explored.[27,45] The surface charge provided by the inherent electrical polarization of the materials has been shown to kill bacteria by destroying the cell wall upon contact. These materials showed a reduction in bacterial load of up to 70% over surfaces[28] and up to 99% in the planktonic state.[29] This reduction of bacterial activity depends on the bacterial strain and bacterial cell membrane type.[30] Previous studies solely relied on polarized surfaces to generate the antibacterial effect or used stimulation provided by mechanical vibration or ultrasound. They did not consider direct low-frequency mechanical stimulation that could be harvested from human movements such as mastication or ambulation, depending on the material's biomedical application.

For the first time, our work shows the effect of piezoelectric charges on bacterial reduction using low frequencies that can be found or harvested from natural human motion. We conducted a systematic evaluation showing the relationship between the magnitude of the electrical charges and the amount of BTO on the bacterial reduction. Our results showed that piezoelectric charges offered a reduction in bacterial load

https://doi.org/10.1021/acsami.1c06331
ACS Appl. Mater. Interfaces 2021, 13, 43868−43879

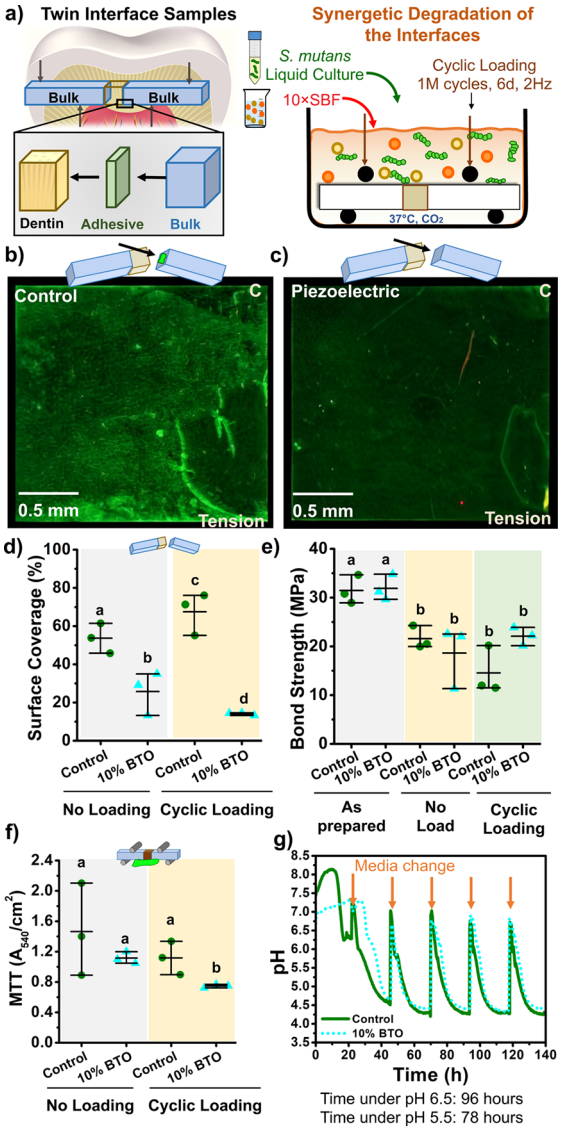

Figure 4. Synergistic model to evaluate the bonding strength of dental composites. (a) Schematic diagram showing the preparation of twin-interface samples and material testing for bonding strength. (b) Representative CLSM image of the fracture surface of a selected control composite under mechanical loading showing bacterial penetration. (c) Representative CLSM image of the fracture surface of a composite filled with 10% BTO under mechanical stimulation. 5% BTO was added to the dental adhesive. Samples were stained with Syto-9 (green) and propidium iodide (red) to indicate live and dead bacteria, respectively. (d) Quantification of the surface coverage by bacteria in control and piezoelectric composites under bacterial attacks (no loading) and bacterial attacks and concomitant cyclic mechanical loading (cyclic loading). (e) Comparison of the residual bond strength for samples subjected to different challenges, including bacterial attacks (no loading), and concomitant bacterial attacks and cyclic mechanical loading (cyclic loading). Values are compared with samples measured after preparation. All samples were challenged for a 6-day period (~1 M cycles). (f) Metabolic activity of *S. mutans* biofilms on twin-interface samples of composites under bacterial attacks (no loading) and concomitant bacterial attacks and cyclic mechanical loading (cyclic loading). $N = 3$ samples for each group and evaluation. Horizontal lines correspond to the minimum, mean, and maximum values. Means with different letters are significantly different ($p \leq 0.05$). (g) Change in the pH over time during the biofilm challenge for control and piezoelectric composite samples.

of up to 90% over biomaterial surfaces, which is higher than that obtained by polarized surfaces (~70%) without cyclic mechanical stimulation.[28]

Our work also shows an optimal antibacterial efficacy that may be achieved with concentrations of BTO between 1 and 10% and when the generated electrical charge is lower than 3.2 pC/cm^2. The antimicrobial effect was not observed in samples without mechanical stimulation of the piezoelectric fillers due to the matrix's high electrical insulating properties (BisGMA/TEGDMA) (Figure 2b,c). However, once the piezoelectric fillers are activated (*i.e.*, charges generated), the antimicrobial activity is observed regardless of the amount of BTO (1–60%), magnitude, or sign of electrical charges (Figure 2d–f). The observed reduction in the biofilm ranged between 50% for the positive surface and 90% on the opposing surface in samples filled with 10% BTO. These results confirm and extend previous studies regarding electrical charges on bacterial viability and biofilm formation.[46] Both positive and negative electrical charges offer an antibacterial effect on Gram-positive and Gram-negative bacteria.[47] It has been reported that piezoelectric ceramics have an antibacterial ratio of almost 100% on positively charged surfaces with positive charges against *S. aureus*.[48]

Electrostatic forces are among the earliest interactions that influence bacterial cells' attachment onto surfaces.[49] Bacteria can adhere to a surface by direct adhesion with the cell wall or binding through the extracellular matrix.[50] The antimicrobial mechanism of electrically charged surfaces is supposedly derived from positive and negative electrical charges with negatively charged sites on the bacterial membrane. The bacterial inactivation may be due to the electrolysis of molecules on bacterial cells' surface, which gives rise to toxic substances such as H_2O_2, chlorine molecules, and oxidizing radicals.[51] Our results suggest that the antimicrobial mechanism of piezoelectric charges is similar. At the onset of mechanical stimulation, piezoelectric charges are generated on the surface of the composite that will create electrostatic interactions, resulting in the repulsion of bacteria and prevention of further adhesion, which eventually inhibits the biofilm growth. These electrical charges also promote ROS generation in the cells that could adhere to the material (Figure 2g). ROS such as superoxide anion (O_2^-), hydrogen peroxide (H_2O_2), hydroxyl radicals (OH^-), lipid hydroperoxides, and singlet oxygen (O_2^1) are species of oxygen produced in all aerobic cells as products or byproducts of metabolic redox reactions.[52]

An increase in ROS that exceeds the cell's antioxidant capability produces oxidative stress within the bacteria, damaging lipids, proteins, and DNA and eventually causing cell death.[52] *S. mutans* is a facultative anaerobe with limited tolerance to ROS and oxidative stresses.[53] Its tolerance to ROS has been reported to depend on the bacterial strain and its specific phenotypic characteristics.[54] The amount of ROS production (mainly hydroxyl radicals and superoxide anions in the CellROX test) by *S. mutans* biofilms cultivated on loaded piezoelectric composites was significantly higher than that in control samples (Figure 2g). The maximum ROS production was observed for composites filled with 10% BTO, which agrees with the maximum reduction of the metabolic activity (Figure 2f). This result suggests that the antibiofilm response of the piezoelectric composites depends on the combination of BTO concentration and magnitude of electrical charge. The antibacterial-mediated killing of bacteria involves oxidative

https://doi.org/10.1021/acsami.1c06331
ACS Appl. Mater. Interfaces 2021, 13, 43868–43879

stress by accumulating superoxide anions and reactive oxygen species. The production of toxic substances [*e.g.*, ROS or reactive chlorine species (RCSs)] has been previously described as the mechanism of action for the bactericidal effect of negative and positive electrical charges.[55] For example, an increase in the ROS levels of *S. aureus* caused by polarization charges has an antibacterial ratio of nearly 100% on the surface of piezoelectric ceramics.[56] However, additional studies regarding the effect of positive and negative electrical charges on ROS production are required.

4.2. Mineralization Effects of Piezoelectric Resin Composites. Negatively charged surfaces accelerate the nucleation and growth of apatite from saturated solutions.[57] Electrostatic interactions attract oppositely charged ions (such as Ca^{2+} and PO_4^{3-}) onto the surface to induce mineralization (heterogeneous nucleation).[57] Different surfaces treated with anionic functional groups (*e.g.*, carboxyl), charged amino acids, and phospholipids have been used for mineralization.[58] Our recent work utilized this powerful mechanism to create materials with self-stiffening properties.[24] This work aimed to utilize piezoelectric charges in a new resin system for remineralization and bond strength improvement.

Overall, increased mineralization was found for the samples with a higher BTO content and surface charge. The piezoelectric resin composite rendered, on average, a mineral growth rate of ~3.3 μm/day for 10× SBF solutions. This rate doubles the one observed by Yamashita *et al.* (1.7 μm/day).[59] We also found that higher concentrations of calcium in SBF (10× SBF) resulted in faster mineral formation (~3.3 μm/day) compared to less-concentrated solutions (1×) (~1.6 μm/day), as previously reported.[24] In the absence of piezoelectric charges (not loaded piezoelectric composites and control samples), there were minerals deposited on the surfaces as dispersed spheroid particles with a diameter up to 1 μm. This mineral morphology is a characteristic of minerals nucleated/precipitated from the bulk SBF solution (not at the material surface).[60] This spontaneous precipitation of calcium phosphates is known as homogeneous nucleation.[60]

Mineral formation using SBF solutions is governed not only by the material's surface chemistry but also by the parameters of the immersion liquid, such as the composition and concentration of the SBF, ionic strength, pH, temperature, and immersion time.[61] The spontaneous precipitation of minerals precedes the apatite phase's formation with higher Ca/P ratios and lower levels of HPO_4^{2-}.[62] Elemental analysis of the minerals formed on the piezoelectric composites exhibited a Ca/P molar ratio of 1.86. Higher Ca/P corresponds to higher substitutions of carbonate for phosphate groups in the precipitated apatite.[63] Negative charges provide more nucleation sites for the positively charged Ca^{2+} ions than surfaces without any charge. As the Ca^{2+} ions accumulate, the material surface becomes positive and can attract and combine with the negatively charged PO_4^{3-} ions of the SBF, forming a layer of calcium phosphate minerals[64] (Figure 3e). Metastable calcium phosphates in SBF transform into a crystalline structure, usually hydroxyapatite and α- or β-tricalcium phosphates.[65]

4.3. Synergetic Degradation of the Bonded Interfaces. Assessing the bond strength of resin composites to dental hard tissues is a known challenge with multiple approaches developed over the years.[66] A major concern is that bond strength tests conducted in the laboratory (*i.e.*, *in vitro*) do not accurately predict the actual clinical performance of dental restorations.[12,67] In addition, there is no model available to study the performance of dental restorations *in vivo*.[68] Thus, developing novel approaches to study restoration performance *in vitro* is necessary. The main reason is that replicating the complex bacteria- and enzyme-rich environment in combination with cyclic mastication forces in lab settings remains difficult.[1] In the oral cavity, multiple degradative challenging factors may be present concomitantly and contribute synergistically to the degradation process of the bonded interfaces. Mimicking these realistic biodegradative synergisms in a laboratory setting has been challenging and is rarely attempted.[12] Current approaches to evaluate the effects of chemical, biological, and mechanical degradation factors on the bond strength commonly study each factor in sequence, independently or separately.[10,32,41,69] In this work, we utilized a dynamic biofilm−fatigue simulator to evaluate, for the first time, the degradation of dentin/adhesive/composite interfaces under the simultaneous attacks from cyclic mechanical loading and bacterial biofilms.

Our results indicate that cyclic loading enabled bacteria to penetrate and cover the bonded interface in the control composites (Figure 4b and Supporting Information-10). Bacteria covered 65 and 50% of the biointerface following cyclic loading or nonloading, respectively. These findings are in agreement with similar studies.[70] Cyclic mechanical loading facilitates bacterial penetration at the dentin restoration margin, which may be due to a hydraulic pumping effect (interface closes/opens repetitively, helping to bring bacterial cells and media inside the interface) and/or demineralization of dentin that facilitates the generation of gaps that fill with media and cells. The antimicrobial effect of piezoelectric charges is evident since only insignificant amounts of bacteria penetrated the biointerface, occupying only ~15% of the fracture surface in the cyclic loading sample.

Despite the absence of bacteria at the interface, the residual bond strengths of the piezoelectric composite and controls during the simultaneous cyclic loading and bacterial attacks were essentially similar. To explain this similarity, we checked the bacterial metabolic activity at the interface (Figure 4f). Piezoelectric composites reduced the metabolic activity of the bacteria at the tension side of the sample. However, the reduction (35%) was not as high as for bulk 10% BTO composites (Figure 2d), presumably due to the tension stresses activating the piezoelectric (antibacterial) charges. The reduction in the metabolic activity in combination with the live/dead staining on the fracture surface (Figure 4c) confirms that the antibacterial effect operates at the interface.

However, the media's pH was <5.5 for 55% of the duration of the experiment and <6.5 for 68% (Figure 4g). Regardless of whether they were cyclically loaded or not, samples were submerged in this medium, and such low pH values may cause demineralization at the outer surfaces of dentin. As a result, the dentin−adhesive area/interface may be externally debilitated by gaps and demineralization and made unnecessary by the bacteria at the bonded interface.[71] Additionally, the cyclic mechanical stress magnitude was 75% lower than the endurance limit for this degradative configuration.[22] As a result, the potential damage and contribution of mechanical stress to reduce the bond strength in this scenario may be insufficient to yield a significant bond strength reduction.

The media used in these experiments were replenished with 5% sucrose three times a day. This formulation was chosen to represent an extreme highly cariogenic diet to ensure a faster

https://doi.org/10.1021/acsami.1c06331
ACS Appl. Mater. Interfaces 2021, 13, 43868−43879

degradation of the bonded interface.[72] Higher concentrations of sucrose lead to prolonged decreases in pH, enhanced demineralization rates, the shift of the plaque microflora to a more cariogenic one, and enhanced cariogenic potential of *S. mutans* (increased acidogenicity and concentrations of extracellular polysaccharides).[73] Sucrose concentrations >5% could upregulate gene expression related to EPS formation, acid production, and tolerance on *S. mutans* biofilms.[74] We conducted additional preliminary fatigue/biofilm tests utilizing higher stress amplitudes (σ_a = 4 MPa) and sucrose concentrations (20 and 10% five times a day) for faster degradation (see Figure SI-12). However, in this case, the degradation rates were significantly faster, and beams failed at ∼400k cycles for 20% sucrose and ∼722k when 10% sucrose was added. These data indicate a strong correlation between the stress magnitude, sucrose concentration, and pulsation and the reduction in the bond strength that warrants further investigation.

Overall, the flexural modulus and stiffness of the 10% BTO piezoelectric composites (σ_y = 65 MPa, E = 2.5 MPa) were significantly lower than those of the control composites (σ_y = 74 MPa, E = 4.1 MPa). Despite these differences, the bond strength of the dentin−adhesive composites for both groups was similar (∼33 MPa) after sample preparation. The adhesive used in the piezoelectric composite group employed a 5% BTO filler. This quantity was selected based on the influence of the adhesive filler quantity on bond strength (see Supporting Information-13). This verifies that by tuning the bioactive filler quantity in the adhesive and bulk composite, it is possible to obtain bond strength tests comparable to commercial/benchmark values. Future investigations should consider optimizing the mechanical properties of the bulk composite by employing nanoparticle surface treatments (*i.e.*, silanization), varying the particle size and shape, or improving nanoparticle dispersion into the matrix. For example, our supporting work showed that by improving the dispersion of the piezoelectric fillers, the mechanical properties were increased by 30% (see Supporting Information-14).

Despite the significant and exciting results, this study still has limitations. First, the antibacterial effect of 10% BTO composite samples was evaluated for 24 h under continuous cyclic loading stimulation. Clinically, the stimulus derived from mastication for piezoelectric fillers may be stochastic and random. Second, the low pH of the media for prolonged times in the bonding strength tests may be driving the degradation of the dentin−adhesive−composite interfaces more than the bacteria themselves or the cyclic mechanical loading. We believe that this is why we do not see a significant improvement in the bond strength for the antibacterial composites. In future experiments, the sucrose needs to be provided in an external container to prevent the media from having acidic drops in the pH that do not represent clinical cases. Third, the degradation and mineralization rates of the bonded interface have different time scales. Bacterial degradation rates occur in a couple of days, whereas significant mineralization takes weeks. Thus, the duration of the experiment needs to be adjusted for the bioactive therapies to be fully operative.

Finally, an ideal antibacterial material should only kill pathogenic bacteria and not commensal species and mammalian cells. Previous studies suggested that piezoelectric materials can have antibacterial responses without affecting mammalian cell viability.[49] However, an excessive increase in ROS and oxidative stress—a result of the antibacterial mechanism—can trigger an inflammatory response in the cells, which eventually can lead to changes in proliferation and differentiation (Supporting Information-11). Further studies regarding the effects of piezoelectric charges on cellular processes are required.

5. CONCLUSIONS

In this study, we incorporated, for the first time, piezoelectric nanoparticles ($BaTiO_3$) into dental resins and investigated the ability of these composites to suppress pathogenic biofilm growth, promote mineral formation at the dentin−adhesive−composite interfaces, and affect the bond strength. The resulting composite material showed an antibacterial and antibiofilm effect, as evidenced by a substantial reduction in the biofilm biomass, metabolic activity, and several viable bacteria compared to control composites. The best antimicrobial effect was found for lower amounts of BTO (<10%) and small electrical charges (<3.2 pC/cm^2). However, the antibacterial response of the composite can be tuned by varying the filler content and applied mechanical load. Furthermore, the piezoelectric composite showed remineralization capabilities evidenced by the formation of calcium phosphate layers with thicknesses ranging 5−23 μm for mechanically stimulated composites in 7 days. We established an *in vitro* model that subjects bonded interfaces (dentin with adhesive/resin composites) to repetitive loading while being submerged in cultures of microorganisms (*i.e.*, pathogenic bacteria). After a 6-day biofilm/cyclic loading challenge, the incorporation of piezoelectric fillers in the dental−adhesive composites prevented the bacterial penetration on the bonded interface. These results indicate that our new composite has the potential to be used as a dental restorative material with antibiofilm and remineralization capabilities for long-term applications. In terms of a broader impact, the use of piezoelectric nanoparticles as antibiofilm/regeneration biomaterials, first shown in this study, could be translated to other medical fields where the eradication of biofilms on implants is a challenge.

■ ASSOCIATED CONTENT

Supporting Information

The Supporting Information is available free of charge at https://pubs.acs.org/doi/10.1021/acsami.1c06331.

Characterization of the piezoelectric composites including roughness measurements, morphological and chemical characterization, mechanical properties (flexural strength and modulus), electromechanical characterization, degree of conversion (DC), water sorption, solubility, and dimensional change tests, simulated body fluid (SBF) preparation method, metabolic activity of bacteria submerged in 10× SBF plus liquid bacteria media, confocal microscopy of the biointerfaces, tests of cytotoxicity and oxidative response of piezoelectric composites and BTO fillers on mammalian cells, effect of sucrose on the bonding strength of bonded interfaces, influence of the adhesive filler quantity on the bond strength, and influence of the preparation method on the mechanical properties of composites (PDF)

https://doi.org/10.1021/acsami.1c06331
ACS Appl. Mater. Interfaces 2021, 13, 43868−43879

AUTHOR INFORMATION

Corresponding Author

Santiago Orrego − *Department of Oral Health Sciences, Kornberg School of Dentistry, Temple University, Philadelphia, Pennsylvania 19140, United States; Bioengineering Department, College of Engineering, Temple University, Philadelphia, Pennsylvania 19122, United States;* orcid.org/0000-0003-3683-6750; Phone: +1-215-707-3817; Email: sorrego@temple.edu

Authors

Carolina Montoya − *Department of Oral Health Sciences, Kornberg School of Dentistry, Temple University, Philadelphia, Pennsylvania 19140, United States*

Anubhav Jain − *Department of Oral Health Sciences, Kornberg School of Dentistry, Temple University, Philadelphia, Pennsylvania 19140, United States*

Juan José Londoño − *Department of Oral Health Sciences, Kornberg School of Dentistry, Temple University, Philadelphia, Pennsylvania 19140, United States; Bioengineering Research Group (GIB), Department of Mechanical Engineering, Universidad EAFIT, Medellin 050022, Colombia*

Santiago Correa − *Bioengineering Research Group (GIB), Department of Mechanical Engineering, Universidad EAFIT, Medellin 050022, Colombia*

Peter I. Lelkes − *Bioengineering Department, College of Engineering, Temple University, Philadelphia, Pennsylvania 19122, United States;* orcid.org/0000-0003-4954-3498

Mary Anne Melo − *Division of Operative Dentistry, Department of General Dentistry, University of Maryland School of Dentistry, Baltimore, Maryland 21201, United States;* orcid.org/0000-0002-0007-2966

Complete contact information is available at: https://pubs.acs.org/10.1021/acsami.1c06331

Notes

The authors declare no competing financial interest.

ACKNOWLEDGMENTS

This work was supported by the Temple University Maurice Kornberg School of Dentistry's startup fund. We would like to acknowledge support from Dr. Divyashri Baraniya, Dr. Nezar Al-Hebshi, and Dr. Sumant Puri of the Oral Microbiome Laboratory at Temple University. We also would like to thank the students Holley Fok, Jenna Bockman, Casey Rubin, Jiamin Deng, Owen Skriloff, and Noah Horvath, who studied at the Smart Biomaterials Lab during 2019−2020.

REFERENCES

(1) Stewart, C. A.; Finer, Y. Biostable, Antidegradative and Antimicrobial Restorative Systems Based on Host-Biomaterials and Microbial Interactions. *Dent. Mater.* **2019**, *35*, 36−52.

(2) Spencer, P.; Ye, Q.; Park, J.; Topp, E. M.; Misra, A.; Marangos, O.; Wang, Y.; Bohaty, B. S.; Singh, V.; Sene, F.; Eslick, J.; Camarda, K.; Katz, J. L. Adhesive/Dentin Interface: The Weak Link in the Composite Restoration. *Ann. Biomed. Eng.* **2010**, *38*, 1989−2003.

(3) Nedeljkovic, I.; De Munck, J.; Vanloy, A.; Declerck, D.; Lambrechts, P.; Peumans, M.; Teughels, W.; Van Meerbeek, B.; Van Landuyt, K. L. Secondary Caries: Prevalence, Characteristics, and Approach. *Clin. Oral Invest.* **2020**, *24*, 683−691.

(4) Mjör, I. A. Clinical Diagnosis of Recurrent Caries. *J. Am. Dent. Assoc.* **2005**, *136*, 1426−1433.

(5) FDI World Dental Federation. Dental Amalgam Phase Down. *Int. Dent. J.* **2019**, *69*, 21−22.

(6) Bourbia, M.; Ma, D.; Cvitkovitch, D. G.; Santerre, J. P.; Finer, Y. Cariogenic Bacteria Degrade Dental Resin Composites and Adhesives. *J. Dent. Res.* **2013**, *92*, 989−994.

(7) Koin, P. J.; Kilislioglu, A.; Zhou, M.; Drummond, J. L.; Hanley, L. Analysis of the Degradation of a Model Dental Composite. *J. Dent. Res.* **2008**, *87*, 661−665.

(8) Mazzoni, A.; Tjäderhane, L.; Checchi, V.; Di Lenarda, R.; Salo, T.; Tay, F. R.; Pashley, D. H.; Breschi, L. Role of Dentin MMPs in Caries Progression and Bond Stability. *J. Dent. Res.* **2015**, *94*, 241−251.

(9) Chien, Y.-C.; Burwell, A. K.; Saeki, K.; Fernandez-Martinez, A.; Pugach, M. K.; Nonomura, G.; Habelitz, S.; Ho, S. P.; Rapozo-Hilo, M.; Featherstone, J. D.; Marshall, S. J.; Marshall, G. W. Distinct Decalcification Process of Dentin by Different Cariogenic Organic Acids: Kinetics, Ultrastructure and Mechanical Properties. *Arch. Oral Biol.* **2016**, *63*, 93−105.

(10) Carrera, C. A.; Li, Y.; Chen, R.; Aparicio, C.; Fok, A.; Rudney, J. Interfacial Degradation of Adhesive Composite Restorations Mediated by Oral Biofilms and Mechanical Challenge in an Extracted Tooth Model of Secondary Caries. *J. Dent.* **2017**, *66*, 62−70.

(11) Daneshkazemi, A.; Davari, A.; Akbari, M. J.; Davoudi, A.; Badrian, H. Effects of Thermal and Mechanical Load Cycling on the Dentin Microtensile Bond Strength of Single Bond-2. *J. Int. Oral Health* **2015**, *7*, 9.

(12) Ferracane, J. L.; Lohbauer, U.; Palin, W. M. The Mechanical Behavior of the Material-Tissue and Material-Material Interface in Dental Reconstructions. *Int. J. Adhes. Adhes.* **2016**, *69*, 2−14.

(13) Mehdawi, I.; Neel, E. A. A.; Valappil, S. P.; Palmer, G.; Salih, V.; Pratten, J.; Spratt, D. A.; Young, A. M. Development of Remineralizing, Antibacterial Dental Materials. *Acta Biomater.* **2009**, *5*, 2525−2539.

(14) Jiao, Y.; Tay, F. R.; Niu, L.-n.; Chen, J.-h. Advancing Antimicrobial Strategies for Managing Oral Biofilm Infections. *Int. J. Oral Sci.* **2019**, *11*, 28.

(15) Makvandi, P.; Jamaledin, R.; Jabbari, M.; Nikfarjam, N.; Borzacchiello, A. Antibacterial Quaternary Ammonium Compounds in Dental Materials: A systematic Review. *Dent. Mater.* **2018**, *34*, 851−867.

(16) Makvandi, P.; Gu, J. T.; Zare, E. N.; Ashtari, B.; Moeini, A.; Tay, F. R.; Niu, L.-n. Polymeric and Inorganic Nanoscopical Antimicrobial Fillers in Dentistry. *Acta Biomater.* **2020**, *101*, 69−101.

(17) Zhang, L.; Weir, M. D.; Chow, L. C.; Antonucci, J. M.; Chen, J.; Xu, H. H. K. Novel Rechargeable Calcium Phosphate Dental Nanocomposite. *Dent. Mater.* **2016**, *32*, 285−293.

(18) Fugolin, A. P. P.; Pfeifer, C. S. New Resins For Dental Composites. *J. Dent. Res.* **2017**, *96*, 1085−1091.

(19) Cheng, L.; Zhang, K.; Weir, M. D.; Melo, M. A. S.; Zhou, X.; Xu, H. H. Nanotechnology Strategies for Antibacterial and Remineralizing Composites and Adhesives to Tackle Dental Caries. *Nanomedicine* **2015**, *10*, 627−641.

(20) Sauro, S.; Pashley, D. H. Strategies to stabilise dentine-bonded interfaces through remineralising operative approaches - State of The Art. *Int. J. Adhes. Adhes.* **2016**, *69*, 39−57.

(21) Tammaro, L.; Di Salle, A.; Calarco, A.; De Luca, I.; Riccitiello, F.; Peluso, G.; Vittoria, V.; Sorrentino, A. Multifunctional Bioactive Resin for Dental Restorative Materials. *Polymers* **2020**, *12*, 332.

(22) Melo, M. A.; Orrego, S.; Weir, M. D.; Xu, H. H. K.; Arola, D. D. Designing Multiagent Dental Materials for Enhanced Resistance to Biofilm Damage at the Bonded Interface. *ACS Appl. Mater. Interfaces* **2016**, *8*, 11779−11787.

(23) Montoya, C.; Du, Y.; Gianforcaro, A. L.; Orrego, S.; Yang, M.; Lelkes, P. I. On the Road to Smart Biomaterials for Bone Research: Definitions, Concepts, Advances, and Outlook. *Bone Res.* **2021**, *9*, 12.

(24) Orrego, S.; Chen, Z.; Krekora, U.; Hou, D.; Jeon, S. Y.; Pittman, M.; Montoya, C.; Chen, Y.; Kang, S. H. Bioinspired Materials with Self-Adaptable Mechanical Properties. *Adv. Mater.* **2020**, *32*, No. e1906970.

(25) Lin, B.; Giurgiutiu, V.; Pollock, P.; Xu, B.; Doane, J. Durability and Survivability of Piezoelectric Wafer Active Sensors on Metallic Structure. *AIAA J.* **2010**, *48*, 635−643.
(26) Buschang, P. H.; Hayasaki, H.; Throckmorton, G. S. Quantification of Human Chewing-Cycle Kinematics. *Arch. Oral Biol.* **2000**, *45*, 461−474.
(27) Marin, E.; Boschetto, F.; Sunthar, T. P. M.; Zanocco, M.; Ohgitani, E.; Zhu, W.; Pezzotti, G. Antibacterial Effects of Barium Titanate Reinforced Polyvinyl-Siloxane Scaffolds. *Int. J. Polym. Mater. Polym. Biomater.* **2021**, *70*, 425−436.
(28) Swain, S.; Padhy, R. N.; Rautray, T. R. Polarized Piezoelectric Bioceramic Composites Exhibit Antibacterial Activity. *Mater. Chem. Phys.* **2020**, *239*, 122002.
(29) Pang, S.; He, Y.; Zhong, R.; Guo, Z.; He, P.; Zhou, C.; Xue, B.; Wen, X.; Li, H. Multifunctional ZnO/TiO2 Nanoarray Composite Coating with Antibacterial Activity, Cytocompatibility and Piezoelectricity. *Ceram. Int.* **2019**, *45*, 12663−12671.
(30) Shah, A. A.; Khan, A.; Dwivedi, S.; Musarrat, J.; Azam, A. Antibacterial and Antibiofilm Activity of Barium Titanate Nanoparticles. *Mater. Lett.* **2018**, *229*, 130−133.
(31) Waller, D.; Safari, A. Corona Poling of PZT Ceramics and Flexible Piezoelectric Composites. *Ferroelectrics* **1988**, *87*, 189−195.
(32) Orrego, S.; Melo, M. A.; Lee, S. H.; Xu, H. H. K.; Arola, D. D. Fatigue of Human Dentin by Cyclic Loading and During Oral Biofilm Challenge. *J. Biomed. Mater. Res., Part B* **2017**, *105*, 1978−1985.
(33) Banas, J. A.; Drake, D. R. Are the mutans streptococci still Considered Relevant to Understanding the Microbial Etiology of Dental Caries? *BMC Oral Health* **2018**, *18*, 129.
(34) Surwit, R. S.; Feinglos, M. N.; McCaskill, C. C.; Clay, S. L.; Babyak, M. A.; Brownlow, B. S.; Plaisted, C. S.; Lin, P. H. Metabolic and Behavioral Effects of a High-Sucrose Diet During Weight Loss. *Am. J. Clin. Nutr.* **1997**, *65*, 908−915.
(35) Ausiello, P.; Ciaramella, S.; Martorelli, M.; Lanzotti, A.; Gloria, A.; Watts, D. C. CAD-FE Modeling and Analysis of Class II Restorations Incorporating Resin-Composite, Glass Ionomer and Glass Ceramic Materials. *Dent. Mater.* **2017**, *33*, 1456−1465.
(36) Camilleri, J.; Arias Moliz, T.; Bettencourt, A.; Costa, J.; Martins, F.; Rabadijeva, D.; Rodriguez, D.; Visai, L.; Combes, C.; Farrugia, C.; Koidis, P.; Neves, C. Standardization of Antimicrobial Testing of Dental Devices. *Dent. Mater.* **2020**, *36*, e59−e73.
(37) Wang, G.; Jin, W.; Qasim, A. M.; Gao, A.; Peng, X.; Li, W.; Feng, H.; Chu, P. K. Antibacterial Effects of Titanium Embedded with Silver Nanoparticles Based on Electron-Transfer-Induced Reactive Oxygen Species. *Biomaterials* **2017**, *124*, 25−34.
(38) Kokubo, T.; Takadama, H. How Useful is SBF in predicting in vivo Bone Bioactivity? *Biomaterials* **2006**, *27*, 2907−2915.
(39) Seemann, R.; Bizhang, M.; Klück, I.; Loth, J.; Roulet, J.-F. A Novel in vitro Microbial-Based Model for Studying Caries Formation - Development and Initial Testing. *Caries Res.* **2005**, *39*, 185−190.
(40) Van Houte, J.; Green, D. B. Relationship Between the Concentration of Bacteria in Saliva and the Colonization of Teeth in Humans. *Infect. Immun.* **1974**, *9*, 624−630.
(41) Arola, D. Fatigue Testing of Biomaterials and their Interfaces. *Dent. Mater.* **2017**, *33*, 367−381.
(42) Koju, N.; Sikder, P.; Ren, Y.; Zhou, H.; Bhaduri, S. B. Biomimetic Coating Technology for Orthopedic Implants. *Curr. Opin. Chem. Eng.* **2017**, *15*, 49−55.
(43) Saeidi, B.; Derakhshandeh, M. R.; Delshad Chermahini, M.; Doostmohammadi, A. Novel Porous Barium Titanate/Nano-bioactive Glass Composite with High Piezoelectric Coefficient for Bone Regeneration Applications. *J. Mater. Eng. Perform.* **2020**, *29*, 5420.
(44) Busuioc, C.; Voicu, G.; Jinga, S.-I.; Mitran, V.; Cimpean, A. The influence of Barium Titanate on the Biological Properties of Collagen-Hydroxiapatite Composite Scaffolds. *Mater. Lett.* **2019**, *253*, 317−322.
(45) Vatlin, I. S.; Chernozem, R. V.; Timin, A. S.; Chernova, A. P.; Plotnikov, E. V.; Mukhortova, Y. R.; Surmeneva, M. A.; Surmenev, R. A. Bacteriostatic Effect of Piezoelectric Poly-3-Hydroxybutyrate and Polyvinylidene Fluoride Polymer Films under Ultrasound Treatment. *Polymers* **2020**, *12*, 240.
(46) Carvalho, E. O.; Fernandes, M. M.; Padrao, J.; Nicolau, A.; Marqués-Marchán, J.; Asenjo, A.; Gama, F. M.; Ribeiro, C.; Lanceros-Mendez, S. Tailoring Bacteria Response by Piezoelectric Stimulation. *ACS Appl. Mater. Interfaces* **2019**, *11*, 27297−27305.
(47) Gottenbos, B.; Grijpma, D. W.; van der Mei, H. C.; Feijen, J.; Busscher, H. J. Antimicrobial Effects of Positively Charged Surfaces on Adhering Gram-positive and Gram-Negative Bacteria. *J. Antimicrob. Chemother.* **2001**, *48*, 7−13.
(48) Yao, T.; Chen, J.; Wang, Z.; Zhai, J.; Li, Y.; Xing, J.; Hu, S.; Tan, G.; Qi, S.; Chang, Y.; Yu, P.; Ning, C. The Antibacterial Effect of Potassium-Sodium Niobate Ceramics Based on Controlling Piezoelectric Properties. *Colloids Surf., B* **2019**, *175*, 463−468.
(49) Tuson, H. H.; Weibel, D. B. Bacteria-surface interactions. *Soft Matter* **2013**, *9*, 4368−4380.
(50) Ueshima, M.; Tanaka, S.; Nakamura, S.; Yamashita, K. Manipulation of Bacterial Adhesion and Proliferation by Surface Charges of Electrically Polarized Hydroxyapatite. *J. Biomed. Mater. Res.* **2002**, *60*, 578−584.
(51) Merriman, H. L.; Hegyi, C. A.; Albright-Overton, C. R.; Carlos, J., Jr.; Putnam, R. W.; Mulcare, J. A. A Comparison of Four Electrical Stimulation Types on Staphylococcus aureus Growth in vitro. *J. Rehabil. Res. Dev.* **2004**, *41*, 139−146.
(52) Sultana, S. T.; Babauta, J. T.; Beyenal, H. Electrochemical Biofilm Control: A Review. *Biofouling* **2015**, *31*, 745−758.
(53) De Furio, M.; Ahn, S. J.; Burne, R. A.; Hagen, S. J. Oxidative Stressors Modify the Response of Streptococcus mutans to its Competence Signal Peptides. *Appl. Environ. Microbiol.* **2017**, *83*, No. e01345.
(54) Liu, Y.; Palmer, S. R.; Chang, H.; Combs, A. N.; Burne, R. A.; Koo, H. Differential oxidative stress tolerance ofStreptococcus mutansisolates affects competition in an ecological mixed-species biofilm model. *Environ. Microbiol. Rep.* **2018**, *10*, 12−22.
(55) Brinkman, C. L.; Schmidt-Malan, S. M.; Karau, M. J.; Greenwood-Quaintance, K.; Hassett, D. J.; Mandrekar, J. N.; Patel, R. Exposure of Bacterial Biofilms to Electrical Current Leads to Cell Death Mediated in Part by Reactive Oxygen Species. *PLoS One* **2016**, *11*, No. e0168595.
(56) Tan, G.; Wang, S.; Zhu, Y.; Zhou, L.; Yu, P.; Wang, X.; He, T.; Chen, J.; Mao, C.; Ning, C. Surface-Selective Preferential Production of Reactive Oxygen Species on Piezoelectric Ceramics for Bacterial Killing. *ACS Appl. Mater. Interfaces* **2016**, *8*, 24306−24309.
(57) Mann, S.. *Biomineralization: Principles and Concepts in Bioinorganic Materials Chemistry*; Oxford University Press on Demand, 2001; Vol. *5*.
(58) Tofail, S. A. M.; Bauer, J. Electrically Polarized Biomaterials. *Adv. Mater.* **2016**, *28*, 5470−5484.
(59) Yamashita, K.; Oikawa, N.; Umegaki, T. Acceleration and Deceleration of Bone-Like Crystal Growth on Ceramic Hydroxyapatite by Electric Poling. *Chem. Mater.* **1996**, *8*, 2697−2700.
(60) Yu, Y.; Bacsik, Z.; Edén, M. Contrasting In Vitro Apatite Growth from Bioactive Glass Surfaces with that of Spontaneous Precipitation. *Materials* **2018**, *11*, 1690.
(61) Shin, K.; Acri, T.; Geary, S.; Salem, A. K. Biomimetic Mineralization of Biomaterials Using Simulated Body Fluids for Bone Tissue Engineering and Regenerative Medicine. *Tissue Eng., Part A* **2017**, *23*, 1169−1180.
(62) Eanes, E. D.; Meyer, J. L. The Maturation of Crystalline Calcium Phosphates in Aqueous Suspensions At Physiologic pH. *Calcif. Tissue Res.* **1977**, *23*, 259−269.
(63) Chrzanowski, W.; Yeow, W. J.; Rohanizadeh, R.; Dehghani, F. Bone bonding ability-how to measure it? *RSC Adv.* **2012**, *2*, 9214−9223.
(64) Kokubo, T.; Yamaguchi, S. Chemical Surface Modification of a Titanium Scaffold. In *Metallic Foam Bone*; Elsevier, 2017; pp 161−179.
(65) Kim, S.; Ryu, H.-S.; Shin, H.; Jung, H. S.; Hong, K. S. In situ Observation of Hydroxyapatite Nanocrystal Formation from

Amorphous Calcium Phosphate in Calcium-Rich Solutions. *Mater. Chem. Phys.* **2005**, *91*, 500−506.
(66) El Mourad, A. M. Assessment of Bonding Effectiveness of Adhesive Materials to Tooth Structure using Bond Strength Test Methods: A Review of Literature. *Open Dent. J.* **2018**, *12*, 664.
(67) Kim, Y.-K. Relationship Between Laboratory Bond Strengths and Clinical Performance of Dentin Adhesives. *Restor. Dent. Endod.* **2016**, *41*, 341.
(68) Ferracane, J. L. Models of Caries Formation around Dental Composite Restorations. *J. Dent. Res.* **2017**, *96*, 364−371.
(69) Mutluay, M. M.; Zhang, K.; Ryou, H.; Yahyazadehfar, M.; Majd, H.; Xu, H. H. K.; Arola, D. On the Fatigue Behavior of Resin-Dentin Bonds After Degradation By Biofilm. *J. Mech. Behav. Biomed. Mater.* **2013**, *18*, 219−231.
(70) Khvostenko, D.; Salehi, S.; Naleway, S. E.; Hilton, T. J.; Ferracane, J. L.; Mitchell, J. C.; Kruzic, J. J. Cyclic Mechanical Loading Promotes Bacterial Penetration Along Composite Restoration Marginal Gaps. *Dent. Mater.* **2015**, *31*, 702−710.
(71) Do, D.; Orrego, S.; Majd, H.; Ryou, H.; Mutluay, M. M.; Xu, H. H. K.; Arola, D. D. Accelerated Fatigue of Dentin With Exposure To Lactic Acid. *Biomaterials* **2013**, *34*, 8650−8659.
(72) Reinke, S. M. G.; de Campos Lawder, J. A.; Divardin, S.; Raggio, D.; Reis, A.; Loguercio, A. D. Degradation of the resin-dentin bonds after simulated and inhibited cariogenic challenge in an in situ model. *J. Biomed. Mater. Res., Part B* **2012**, *100B*, 1466−1471.
(73) Leme, A. F. P.; Koo, H.; Bellato, C. M.; Bedi, G.; Cury, J. A. The Role of Sucrose in Cariogenic Dental Biofilm Formation-New Insight. *J. Dent. Res.* **2006**, *85*, 878−887.
(74) Cai, J.-N.; Jung, J.-E.; Lee, M.-H.; Choi, H.-M.; Jeon, J.-G. Sucrose Challenges to Streptococcus mutans Biofilms and the Curve Fitting for the Biofilm Changes. *FEMS Microbiol. Ecol.* **2018**, *94*, fiy091.

https://doi.org/10.1021/acsami.1c06331
ACS Appl. Mater. Interfaces 2021, 13, 43868−43879